Bright attosecond soft X-ray pulse trains by transient phase-matching in two-color high-order harmonic generation

Bernd Schütte,[1,6] Paul Weber,[1] Katalin Kovács,[2,3,4] Emeric Balogh,[2,4] Balázs Major,[2] Valer Tosa,[3,4,5] Songhee Han,[1] Marc J J Vrakking,[1] Katalin Varjú,[2,4] and Arnaud Rouzée[1,*]

[1]*Max-Born-Institut, Max-Born-Strasse 2A, 12489 Berlin, Germany*
[2]*Department of Optics and Quantum Electronics, University of Szeged, Szeged, Hungary*
[3]*National Institute for R&D Isotopic and Molecular Technologies, Cluj-Napoca, Romania*
[4]*ELI-ALPS, ELI-Hu Nkft, Szeged 6720, Hungary*
[5]*King Saud University, Riyadh-11451, Saudi Arabia*
[6]*Present address: Department of Physics, Imperial College London, South Kensington Campus, SW7 2AZ London, United Kingdom*

[*]*rouzee@mbi-berlin.de*

Abstract: We study two-color high-order harmonic generation in Neon with 790 nm and 1300 nm driving laser fields and observe an extreme-ultraviolet continuum that extends to photon energies of 160 eV. Using a 6-mm-long, high pressure gas cell, we optimize the HHG yield at high photon energies and investigate the effect of ionization and propagation under phase-matching conditions that allow us to control the temporal structure of the XUV emission. Numerical simulations that include the 3D propagation of the two-color laser pulse show that a bright isolated attosecond pulse with exceptionally high photon energies can be generated in our experimental conditions due to an efficient hybrid optical and phase-matching gating mechanism.

OCIS codes: (140.0140) Lasers and laser optics; (320.0320) Ultrafast optics; (340.0340) X-ray optics.

References and links

1. F. Krausz and M. Ivanov, "Attosecond physics," Rev. Mod. Phys. **81**, 163–234 (2009).
2. F. Lépine, G. Sansone, and M. J. J. Vrakking, "Molecular applications of attosecond laser pulses," Chem. Phys. Lett. **578**, 1–14 (2013).
3. A. Landers, Th. Weber, I. Ali, A. Cassimi, M. Hattass, O. Jagutzki, A. Nauert, T. Osipov, A. Staudte, M. H. Prior, H. Schmidt-Böcking, C. L. Cocke, and R. Dörner, "Photoelectron diffraction mapping: molecules illuminated from within," Phys. Rev. Lett. **87**, 013002 (2001).
4. U. Frühling, M. Wieland, M. Gensch, T. Gebert, B. Schütte, M. Krikunova, R. Kalms, F. Budzyn, O. Grimm, J. Rossbach, E. Plönjes, and M. Drescher, "Single-shot terahertz-field-driven X-ray streak camera," Nat. Photonics **3**, 523-528 (2009).
5. P. Emma, R. Akre, J. Arthur, R. Bionta, C. Bostedt, J. Bozek, A. Brachmann, P. Bucksbaum, R. Coffee, F.-J. Decker, Y. Ding, D. Dowell, S. Edstrom, A. Fisher, J. Frisch, S. Gilevich, J. Hastings, G. Hays, Ph. Hering, Z. Huang, R. Iverson, H. Loos, M. Messerschmidt, A. Miahnahri, S. Moeller, H.-D. Nuhn, G. Pile, D. Ratner, J. Rzepiela, D. Schultz, T. Smith, P. Stefan, H. Tompkins, J. Turner, J. Welch, W. White, J. Wu, G. Yocky, and J. Galayda, "First lasing and operation of an angstrom-wavelength free-electron laser," Nature **4**, 641 (2010).
6. T. Maltezopoulos, S. Cunovic, Ma. Wieland, M. Beye, A. Azima, H. Redlin, M. Krikunova, R. Kalms, U. Frühling, F. Budzyn, W. Wurth, A. Föhlisch, and M. Drescher, "Single-shot timing measurement of extreme-ultraviolet free-electron laser pulses," New J. Phys. **10**, 033026 (2008).

#248407 Received 24 Aug 2015; revised 16 Nov 2015; accepted 16 Nov 2015; published 23 Dec 2015

7. W. Ackermann, G. Asova, V. Ayvazyan, A. Azima, N. Baboi, J. Baehr, V. Balandin, B. Beutner, A. Brandt, A. Bolzmann, R. Brinkmann, O. I. Brovko, M. Castellano, P. Castro, L. Catani, E. Chiadroni, S. Choroba, A. Cianchi, J. T. Costello, D. Cubaynes, J. Dardis, W. Decking, H. Delsim-Hashemi, A. Delserieys, G. Di Pirro, M. Dohlus, S. Duesterer, A. Eckhardt, H. T. Edwards, B. Faatz, J. Feldhaus, K. Floettmann, J. Frisch, L. Froehlich, T. Garvey, U. Gensch, Ch. Gerth, M. Goerler, N. Golubeva, H.-J. Grabosch, M. Grecki, O. Grimm, K. Hacker, U. Hahn, J. H. Han, K. Honkavaara, T. Hott, M. Huening, Y. Ivanisenko, E. Jaeschke, W. Jalmuzna, T. Jezynski, R. Kammering, V. Katalev, E. T. Kavanagh, S. Kennedy, K. Khodyachykh, K. Klose, V. Kocharyan, M. Koerfer, M. Kollewe, W. Koprek, S. Korepanov, D. Kostin, M. Krassilnikov, G. Kube, M. Kuhlmann, C. L. S. Lewis, L. Lilje, T. Limberg, D. Lipka, F. Loehl, H. Luna, M. Luong, M. Martins, M. Meyer, P. Michelato, V. Miltchev, W. D. Moeller, L. Monaco, W. F. O. Mueller, A. Napieralski, O. Napoly, P. Nicolosi, D. Noelle, T. Nunez, A. Oppelt, C. Pagani, R. Paparella, R. Pchalek, N. Pedregosa-Gutierrez, J. Petersen, B. Petrosyan, G. Petrosyan, L. Petrosyan, J. Pflueger, E. Ploenjes, L. Poletto, K. Pozniak, E. Prat, D. Proch, P. Pucyk, P. Radcliffe, H. Redlin, K. Rehlich, M. Richter, M. Roehrs, J. Roensch, R. Romaniuk, M. Ross, J. Rossbach, V. Rybnikov, M. Sachwitz, E. L. Saldin, W. Sandner, H. Schlarb, B. Schmidt, M. Schmitz, P. Schmueser, J. R. Schneider, E. A. Schneidmiller, S. Schnepp, S. Schreiber, M. Seidel, D. Sertore, A. V. Shabunov, C. Simon, S. Simrock, E. Sombrowski, A. A. Sorokin, P. Spanknebel, R. Spesyvtsev, L. Staykov, B. Steffen, F. Stephan, F. Stulle, H. Thom, K. Tiedtke, M. Tischer, S. Toleikis, R. Treusch, D. Trines, I. Tsakov, E. Vogel, T. Weiland, H. Weise, M. Wellhoeffer, M. Wendt, I. Will, A. Winter, K. Wittenburg, W. Wurth, P. Yeates, M. V. Yurkov, I. Zagorodnov, and K. Zapfe, "Operation of a free-electron laser from the extreme ultraviolet to the water window," Nat. Photonics **1**, 336 (2007).
8. T. Popmintchev, M.-C. Chen, D. Popmintchev, P. Arpin, S. Brown, S. Alisauskas, G. Andriukaitis, T. Balciunas, O. D. Mücke, A. Pugzlys, A. Baltuska, B. Shim, S. E. Schrauth, A. Gaeta, C. Hernandez-Garcia, L. Plaja, A. Becker, A. Jaron-Becker, M. M. Murnane, and H. C. Kapteyn, "Bright coherent ultrahigh harmonics in the keV X-ray regime from mid-infrared femtosecond lasers," Nat. Photonics **336**, 1287 (2012).
9. M-C. Chen, C. Mancuso, C. Hernandez-Garcia, F. Dollar, B. Galloway, D. Popmintchev, P. Huang, B. Walker, L. Plaja, A. A. Jaron-Becker, A. Becker, M. M. Murnane, H. C. Kapteyn, and T. Popmintchev, "Generation of bright isolated attosecond Soft X-Ray pulses driven by multi-cycle mid-infrared lasers," Proc. Natl. Acad. Sci. U. S. A. **111**, E2361 (2014).
10. C. Ding, W. Xiong, T. Fan, D. D. Hickstein, T. Popmintchev, X. Zhang, M. Walls, M. Murnane, and H. C. Kapteyn, "High flux coherent supercontinuum soft X-ray source driven by a single-stage 10 mJ, kHz, Ti: sapphire laser amplifier," Opt. Express **22**, 6194 (2014).
11. J. Tate, T. Auguste, H. G. Muller, P. Salieres, P. Agostini, and L. F. DiMauro, "Scaling of wave-packet dynamics in an intense midinfrared field," Phys. Rev. Lett. **98**, 013901 (2007).
12. G. Tempea, M. Geissler, M. Schnürer, and T. Brabec, "Self-phase-matched high harmonic generation," Phys. Rev. Lett. **84**, 4329 (2000).
13. C. Siedschlag, H. G. Muller, and M. J. J. Vrakking, "Generation of isolated attosecond pulses by two-color laser fields," Laser Phys. **15**, 916 (2005).
14. C. Vozzi, F. Calegari, F. Frassetto, L. Poletto, G. Sansone, P. Villoresi, M. Nisoli, S. De Silvestri, and S. Stagira, "Coherent continuum generation above 100 eV driven by an IR parametric source in a two-color scheme," Phys. Rev. A **79**, 033842 (2009).
15. F. Calegari, C. Vozzi, M. Negro, G. Sansone, F. Frassetto, L. Poletto, P. Villoresi, M. Nisoli, S. De Silvestri, and S. Stagira, "Efficient continuum generation exceeding 200 eV by intense ultrashort two-color driver," Opt. Lett. **34**, 3125 (2009).
16. T. Siegel, R. Torres, D. J. Hoffmann, L. Brugnera, I. Procino, A. Zaïr, Jonathan G. Underwood, E. Springate, I. C. E. Turcu, L. E. Chipperfield, and J. P. Marangos, "High harmonic emission from a superposition of multiple unrelated frequency fields," Opt. Express **18**, 6853 (2010).
17. E. J. Takahashi, P. Lan, O. D. Mücke, Y. Nabekawa, and K. Midorikawa, "Infrared two-color multicycle laser field synthesis for generating an intense attosecond pulse," Phys. Rev. Lett. **104**, 233901 (2010).
18. P. Lan, E. J. Takahashi, and K. Midorikawa, "Optimization of infrared two-color multicycle field synthesis for intense-isolated-attosecond-pulse generation," Phys. Rev. A **82**, 053413 (2010).
19. T. Pfeifer, L. Gallmann, M. J. Abel, P. M. Nagel, D. M. Neumark, and S. R. Leone, "Heterodyne mixing of laser fields for temporal gating of high-order harmonic generation," Phys. Rev. Lett. **97**, 163901 (2006).
20. E. Balogh, K. Kovacs, P. Dombi, J. A. Fulop, G. Farkas, J. Hebling, V. Tosa, and K. Varju, "Single attosecond pulse from terahertz-assisted high-order harmonic generation," Phys. Rev. A **84**, 023806 (2011).
21. V. Tosa, C. Altucci, K. Kovacs, N. Negro, S. Stagira, C. Vozzi, and R. Velotta, "Gating of high-order harmonics generated by incommensurate two-color mid-IR laser pulses," IEEE J. Sel. Top. Quantum Electron. **18**, 239 (2012).
22. E. J. Takahashi, P. Lan, O. D. Mucke, Y. Nabekawa, and K. Midorikawa, "Attosecond nonlinear optics using gigawatt-scale isolated attosecond pulses," Nat. Commun. **4**, 2691 (2013).
23. G. Gademann, F. Ple, P-M. Paul, and M. J. J. Vrakking, "Carrier-envelope phase stabilization of a terawatt level chirped pulse amplifier for generation of intense isolated attosecond pulses," Opt. Express **19**, 24922 (2011).
24. E. Constant, D. Garzella, P. Breger, E. Mevel, C. Dorrer, C. Le Blanc, F. Salin, and P. Agostini, "Optimizing high harmonic generation in absorbing gases: Model and experiment," Phys. Rev. Lett. **82**, 1668 (1999).

#248407 Received 24 Aug 2015; revised 16 Nov 2015; accepted 16 Nov 2015; published 23 Dec 2015

25. E. Priori, G. Cerullo, M. Nisoli, S. Stagira, S. De Silvestri, P. Villoresi, L. Poletto, P. Ceccherini, C. Altucci, R. Bruzzese, and C. de Lisio, "Nonadiabatic three-dimensional model of high-order harmonic generation in the few-optical-cycle regime," Phys. Rev. A **61**, 063801 (2000).
26. M. Lewenstein, P. Salières, and A. l'Huilier, "Theory of high-harmonic generation by low-frequency laser fields," Phys. Rev. A **61**, 063801 (2000).
27. H. Kim, I. Kim, V. Tosa, Y. Lee, and C. Nam, "Gating of high-order harmonics generated by incommensurate two-color mid-IR laser pulses," App. Phys. B **78**, 863 (2004).
28. V. Tosa, E. Balogh, and K. Kovacs, "Phase-matched generation of water-window X-rays," Phys. Rev. A **80**, 045801 (2009).

1. Introduction

High-order harmonic generation (HHG) is a unique technique allowing the generation of bursts of ultrashort extreme-ultraviolet (XUV) light. These pulses provide a way to study ultrafast electronic processes in matter on their natural time scale down to the attosecond regime [1, 2]. So far, these studies have been, to a large extent, limited to photon energies below 100 eV. To explore inner-shell processes, such as core-shell ionization and Auger emission [3], higher photon energies are necessary. Our current knowledge of inner-shell processes derives primarily from synchrotron experiments, where the pulse durations are too long for time-resolved studies. In contrast, free-electron lasers have pulse durations in the femtosecond range [4] and photon energies up to the keV range [5], but their large timing jitter [6] and shot-to-shot fluctuations [7] make so far pump-probe experiments challenging. Therefore, HHG schemes capable of generating stable ultrashort XUV or X-ray pulses with photon energies above 100 eV at high intensity are desirable, since these sources allow the implementation of pump-probe configurations with ultimate time resolution.

Recently, HHG X-ray sources have been developed using long-wavelength drivers [8–10]. While the scaling of the ponderomotive energy with $I_{laser}\lambda^2$ creates the opportunity for generating keV photon energies, this approach suffers from the λ^{-6} scaling law of the conversion efficiency of the HHG for a "single" atom with the driver wavelength [11]. An improved efficiency can be achieved in a hollow-core waveguide in which phase-matching (PM) is maintained for a long propagation length and high gas pressure. A scheme was as well proposed to extend the phase-matching process to shorter X-ray wavelengths by using the deformation in the electric field of an intense few-cycle laser pulse induced by ionization [12]. Another approach is to apply two-color schemes, where one color is centered around 800 nm and the other color is in the mid-infrared (MIR), typically between 1.2 μm and 1.6 μm [13–17]. Theoretically, it was predicted that the harmonic conversion efficiency scales as λ^{-3} to λ^{-4} in such a two-color configuration [18]. These studies also demonstrated that two-color schemes enable the generation of continuous XUV spectra. When Kr and Ar were used as target media [14, 16, 17], mainly harmonics below 100 eV were generated, while in Ne [15] photons exceeding 200 eV were reported, albeit with only 100 photons/eV/shot at photon energies above 120 eV. With so few photons, photoelectron and -ion spectroscopy in dilute systems is extremely challenging. Theoretical proposals have been made to use heterodyne mixing of two infrared fields with incommensurable wavelengths to drive the generation of isolated bursts of XUV/X-ray light [13, 19–21]. An experimental realization of this idea was recently demonstrated [22] showing the possibility to generate isolated attosecond pulses (IAP)with unprecedented peak power around 30 eV photon energy.

In the present study, we investigate and optimize HHG in Neon exploiting a two-color scheme with driving laser pulses centered at 790 nm and 1300 nm. A significantly higher flux with respect to the experiment reported in [15] is achieved by increasing the number of emitters using a more than three times longer focal length and a long gas cell filled at a relatively high pressure. We observe the generation of a nearly flat soft X-ray continuum between 70 and

#248407 Received 24 Aug 2015; revised 16 Nov 2015; accepted 16 Nov 2015; published 23 Dec 2015

160 eV. Numerical simulations reproduce the measured spectra and indicate the presence of a bright IAP due to efficient hybrid optical and phase-matching gating.

2. Experimental setup

The experiments were performed using a Ti:sapphire laser with a central near-infrared (NIR) wavelength of 790 nm, a pulse energy of 35 mJ and a pulse duration of 32 fs, operating at a repetition rate of 50 Hz [23]. 25 mJ of the pulse energy was coupled into a commercial high conversion optical parametric amplifier (HE-TOPAS-prime) in order to generate up to 4 mJ of MIR light at a wavelength of 1.3 μm. Up to 6 mJ of the remaining pulse energy was used as the fundamental driver for the HHG process. The NIR and MIR pulses were combined using a 45° dichroic mirror and focused into a 6 mm long gas cell statically filled with Neon. For the focusing, a spherical mirror with a 50 cm long focal length was used. The delay of the NIR pulse with respect to the MIR pulse was adjusted by a computer-controlled motorized delay stage, and the polarization of the two beams was set parallel. To achieve similar focus sizes for both beams, the MIR beam waist diameter was adjusted using a telescope, resulting in a beam waist of 50 μm for both beams. The NIR and MIR pulse durations on target were estimated to be 50 fs, full-width-half-maximum. After the HHG conversion process, a Zr filter was used to block the remaining NIR and MIR pulses, while harmonics between 70 eV and 200 eV were transmitted. A concave grating with a variable-line-spacing was employed to disperse the XUV beam towards a multichannel plate/phosphor screen assembly, where spectra were recorded with a CCD camera.

3. Results

3.1. Experimental results

Single-color high harmonic spectra recorded experimentally in Neon atoms for both driving wavelengths separately, i.e. for 790 nm and 1300 nm, are shown in Fig. 1(a). The laser pulse parameters, cell position and gas pressure were optimized in both cases to generate a maximum harmonic yield. An important issue in HHG with longer-wavelength driving fields is the strongly reduced single-atom response, which generally results in a much lower high harmonic yield. For instance, in our experiment, the signal obtained below 100 eV with the 1300 nm driving pulse is two orders of magnitude lower than the corresponding yield obtained with the 790 nm field, as shown Fig. 1(a). However, the cut-off in the 1300 nm spectrum near 210 eV is twice as high as the cut-off in the 790 nm spectrum. One-color HHG using MIR pulses was previously optimized by working at high gas pressures (up to 35 bar) in a long hollow waveguide geometry [8]. In that experiment, the large number of atoms taking part in the HHG process partially compensated for the low single-atom response. Moreover, the large Kerr-effect and plasma generation at high gas pressure was responsible for a self-confinement of the laser beam as it propagated through the medium, which allowed to maintain the PM over a long propagation length [8], and therefore to enhance the HHG yield.

In our experiment, HHG takes place inside a gas cell, i.e. in a non-guiding geometry. However, self-confinement of the laser beams due to Kerr-effect and plasma generation is anticipated in our experimental conditions, i.e. when combining a long gas cell, a high gas pressure and high intensity of the laser pulses. Together with the favorable scaling of the HHG yield with a two-color laser field described in [18], a good conversion efficiency is therefore expected. The harmonic spectrum recorded upon use of two-color 790 nm and 1300 nm laser pulses is displayed in Fig. 1(a). An extended cut-off with respect to the 790 nm case, as well as a significantly increased efficiency with respect to the 1300 nm case in the 100 eV - 160 eV range are observed. Altogether, the two-color HHG using the combination of a high gas pressure and a

#248407 Received 24 Aug 2015; revised 16 Nov 2015; accepted 16 Nov 2015; published 23 Dec 2015

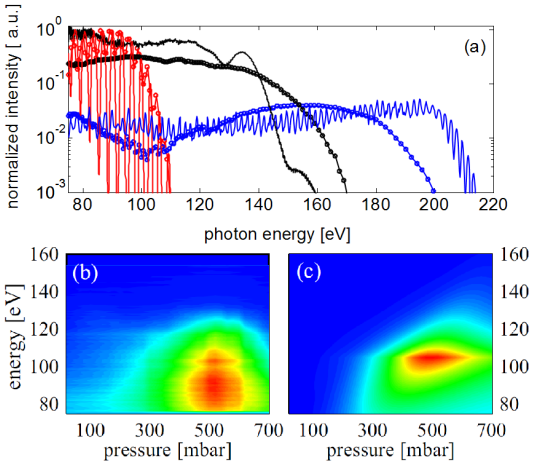

Fig. 1. (a) Experimental high harmonic spectra recorded using a 790 nm NIR laser field with a $5 \cdot 10^{14}$ W/cm^2 peak intensity (red circles), using a 1300 nm MIR laser field with a $6 \cdot 10^{14}$ W/cm^2 peak intensity (blue circles) and a two-color NIR+MIR laser field with a $5 \cdot 10^{14}$ W/cm^2 peak intensity for both pulses for a temporal delay of 0 fs (black circles). All spectra are normalized to the HHG signal generated by the 790 nm pulse. The solid curves are simulated HHG spectra using the 3D model obtained for: a 790 nm NIR laser field with a $7 \cdot 10^{14}$ W/cm^2 peak intensity (red), a 1300 nm MIR laser field with a $7 \cdot 10^{14}$ W/cm^2 peak intensity (blue) and a two-color laser field with a $7 \cdot 10^{14}$ W/cm^2 peak intensity for both pulses (black). The gas cell pressure was 500 mbar in all calculations. (b) Pressure-dependent high harmonic yield recorded experimentally for the two-color laser field. (c) Pressure dependence of single-color (800 nm) HHG, calculated using the 1D model in [24], assuming a 0.8% ionization rate, a cell placed 4 mm before the focus, and a single-atom response with a plateau up to 105 eV, decreasing exponentially in the cut-off.

6-mm-long gas cell allows for the generation of a continuum between 70 eV and 160 eV, with a yield that for photon energies below 100 eV is only reduced by a factor of 3 with respect to the harmonic yield obtained with the 790 nm pulse only. To estimate the HHG flux generated in our experimental conditions, the HHG beam was focused into a gas jet containing xenon atoms and the electron yield resulting from single-photon ionization was recorded. Using known cross-sections for the photoionization of xenon, we estimated that 10^7 photons/eV/pulse and almost 10^9 photons/eV/s were generated, representing an improvement of two to three orders of magnitude in comparison to the results reported in [15].

The optimum conversion efficiency in the two-color HHG was found at 500 mbar [Fig. 1(b)], which is significantly higher than the pressure used in conventional HHG schemes at 790 nm, that use relatively low incident pulse energies. This result is well reproduced by a single-color 1-dimensional (1D) model where the PM between the 790 nm pulse and the generated XUV components was investigated on axis [24] [Fig. 1(c)]. For an ionization rate of 0.8%, which corresponds to the ionization level obtained from our more extensive 3D model for the laser intensity used in the experiment (detailed in the next section), the phase mismatch associated with the plasma dispersion and the Gouy phase shift cancel the phase mismatch associated with the neutral dispersion, and thus minimizes the phase mismatch between the NIR and the generated soft X-ray pulses.

We investigated the effect of changing the intensities of the two laser fields while keeping the same conditions for all the other parameters. The results are shown in Fig. 2, where two-color

#248407 Received 24 Aug 2015; revised 16 Nov 2015; accepted 16 Nov 2015; published 23 Dec 2015

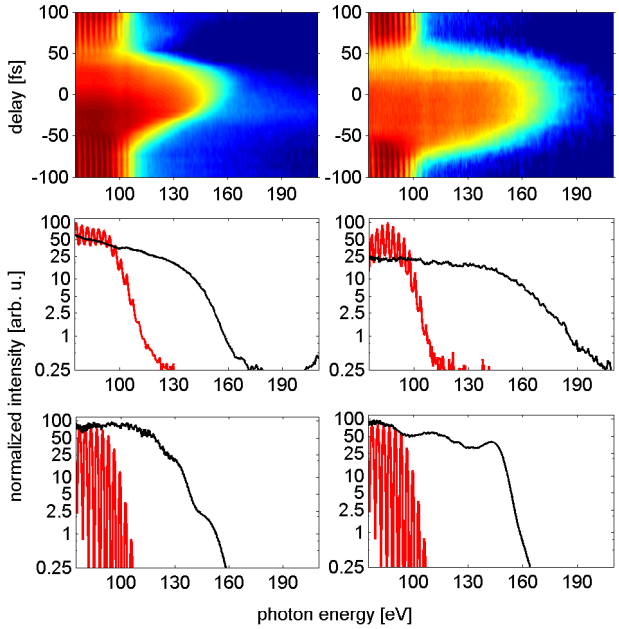

Fig. 2. Two-color HHG spectra recorded in a 6-mm-long cell filled with Ne at a pressure of 500 mbar. Top row: delay scans, where at negative delays the NIR pulse precedes the MIR pulse. Middle row: spectra sampled at -100 fs delay, i.e. NIR-only spectra (red) and at zero delay, thus displaying the longest cut-off extension (black). Bottom row: simulated spectra obtained with the 3D model. The two columns correspond to different combinations of (NIR, MIR) intensities. Left column (5 10^{14} W/cm^2, 1.5 10^{14} W/cm^2), right column (4.5 10^{14} W/cm^2, 5 10^{14} W/cm^2).

delay scans (top panel) and selected spectra recorded well before and at time overlap (middle panel) are presented for two different intensity combinations of the NIR and MIR laser pulses. For the lowest intensities used in our study [Fig. 2 left column], a large increase of the harmonic yield is observed at time overlap together with a cut-off extension from 100 eV (NIR only) to 140 eV (two-color case). We note that for the low MIR laser intensity used, no harmonic signal could be detected with the MIR laser pulse alone. In this intensity configuration, the harmonic yield recorded at time overlap is almost constant over the energy range from 70 to 140 eV, and only decreases by a factor of two with respect to the NIR-only yield below 100 eV. Increasing the MIR laser intensity leads to a cut-off extension up to 160 eV, but at the expense of a decreased yield (right column).

3.2. Simulation results and phase-matching mechanism

In order to understand the optimal conditions for bright coherent emission at higher photon energies, we performed extensive numerical simulations, using a 3D non-adiabatic model. To do so, the model described in [25] was extended [21] in order to treat the two-color configuration. In the simulation the two driving pulses were propagated independently, but they were coupled through the plasma created by the combined field, and through the third order susceptibility of the medium. The atomic dipole induced by the laser field was calculated using the strong field approximation (SFA) [26], and finally the generated harmonics were propagated taking into account their dispersion and absorption. Due to the high intensities and high pressure used

#248407 Received 24 Aug 2015; revised 16 Nov 2015; accepted 16 Nov 2015; published 23 Dec 2015

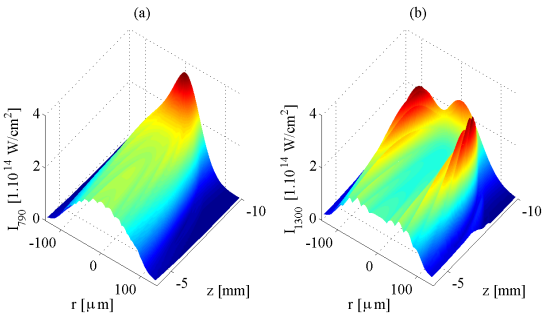

Fig. 3. Evolution of the radial distribution of the 800 nm (a) and 1300 nm (b) beams during propagation in the gas cell. The z coordinate corresponds to the displacement with respect to the laser focus.

in the experiment, significant field distortions occur as the pulses propagate through the long interaction medium. The rapid variation of the refractive index due to ionization on the rising edge of the pulses causes strong self-phase modulation and defocusing and it is important to include these modifications of the driving pulses because the atomic dipole will inherit these distortions. In our model, the variation in amplitudes and phases of the two laser beams as they propagate within the interaction cell are fully taken into account.

Calculations were first benchmarked using the measured single-color HHG spectra. The size of the gas cell and the Neon pressure inside the gas cell were fixed to the experimental values (6 mm, 500 mbar), and the intensity and the position of the cell with respect to the focus were adjusted to best match the experimental results. A comparison of experimental and simulated spectra is given in Fig. 1(a) for both wavelengths showing a good agreement between the HHG spectra recorded experimentally and calculated using the 3D model. For the simulations we have used initially Gaussian pulses with peak intensities 20% higher than the experimental values both for the NIR and the MIR pulses. We expect the difference to originate from a slight overestimation of the beam waist at the focus. The model also satisfactorily reproduces the experimentally recorded two-color HHG spectra [see Figs. 1 and 2]. A large cut-off extension from 100 eV (790 nm laser pulse only) to 160 eV (two-color laser field) is observed, together with a very high harmonic yield that is almost identical to the yield obtained with the 790 nm laser pulse alone. Our simulations confirm therefore that a long gas cell and a high-pressure target, combined with a two-color laser scheme allows for efficient generation of high-harmonics over a large photon energy range extending to 160 eV.

In our simulation, best PM was achieved when the medium was placed before the laser focus, which is known to be the optimum in high ionization [27] or high pressure [28] conditions. In this case the balance between geometrical focusing and plasma defocusing reaches an equilibrium. In the beginning of the propagation, both the NIR and MIR pulses suffer serious reshaping and, after 1 mm propagation, the intensities reach an almost flat profile both in radial and axial directions [see Fig. 3]. Since the phase of harmonics is proportional to the intensity of the driving field I, a slowly varying intensity helps the constructive build-up of harmonics along propagation. The reshaping of the pulses that occurs in the front part of the long gas cell creates therefore a relatively stable intensity and radial profile for the harmonic generation to occur under favorable PM conditions in the latter part of the cell. This behavior was confirmed experimentally by measuring the high harmonic beam profiles generated with the NIR pulse only and with both the NIR and MIR pulses. In the latter case, a large distortion of the beam profile together with a large increase of the beam size (by a factor 1.5) was observed.

Our simulations reveal that the two-color HHG continuum observed experimentally is likely

#248407 Received 24 Aug 2015; revised 16 Nov 2015; accepted 16 Nov 2015; published 23 Dec 2015

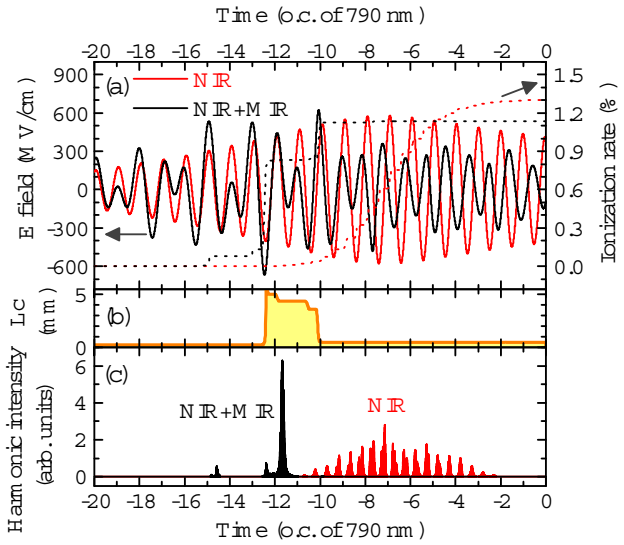

Fig. 4. (a) Rising edge of the single color (solid red curve) and two-color NIR+MIR laser field (solid black curve) after propagation, obtained in our 3D simulation, and the corresponding time evolution of the ionization rate (dotted red and black curves). (b) Coherence length for 100 eV harmonics as a function of time calculated in the 1D model using the ionization rate from the top panel. (c) Temporal shape of the XUV radiation after propagation generated with the two-color NIR+MIR laser field showing the generation of an IAP (black). For comparison, the results for a NIR-only laser field, leading to the production of an attosecond pulse train, are shown as well (red).

to originate from an efficient gating mechanism that leads to IAP generation. A gating mechanism occurs both at the microscopic (single-atom response) and macroscopic (phase-matching) level. First, the periodicity of the two-color HHG process is determined by the least common multiple of the laser periods. Given that the ratio of the wavelengths is approximately 1.6, the two-color HHG process is replicated every 5 optical cycles of the 790 nm laser (correspondingly to 3 optical cycles of the 1300 nm laser). During one such time interval two attosecond pulses are generated, i.e. separated by 2.5 times the 790 nm optical cycle. This alone leads to an increased separation of the attosecond bursts and denser harmonic line structure. Second, macroscopic gating arises during propagation in the ionized medium and can be described as an interplay between temporal and spatial effects. The superposition of the NIR and MIR fields leads to rapid ionization which destroys PM and confines the HHG to a narrow time-window on the rising edge of the laser pulses [see Figs. 4(a) and 4(b)]. This tendency is further strengthened by the fact that ionization reshapes the NIR and MIR laser fields, leading to a pronounced intensity drop in the second half of the pulse. From this, it follows that high energy photons are emitted only in very few events. Note that in this explanation, we are predominantly considering attosecond pulses generated in the last part of the cell since attosecond pulses emitted at the beginning of the cell are efficiently absorbed in the dense medium (the absorption length is around 0.5 mm). Thus our calculations suggest that the combination of the two laser fields in a long, high pressure gas cell assures that only one attosecond pulse is eventually present [Fig. 4(c)]. The PM mechanism gated in a narrow time-window on the rising edge of the driving field was also seen recently in case of HHG using multi-cycle MIR pulses in high density gas medium [9]. We show that in the proposed arrangement, many-cycle pulses (50 fs) can be used

#248407 Received 24 Aug 2015; revised 16 Nov 2015; accepted 16 Nov 2015; published 23 Dec 2015

for IAP production. Due to the larger temporal separation of intense half-cycles in the two-color case, the requirements on the width of the PM window are considerably relaxed. For our 50 fs pulses, the coherence length exceeds a few millimeters for only a few optical cycles [see Fig. 4(b)].

The simulation results presented in Fig. 4 were carried out for an initial relative carrier-envelope phase (CEP) between the NIR and MIR laser fields fixed to $\Delta\phi = 0$. In this condition, an IAP is generated [see Fig. 4(c)]. However, simulations show that not all relative CEPs result in the generation of an isolated attosecond pulse. In our experiment, the carrier-envelope phase of the NIR and MIR laser pulses were not stabilized and our observation of a soft X-ray continuum between 70 and 160 eV can therefore not unambiguously prove the generation of an isolated attosecond pulse. Nevertheless, our simulation suggests that bright attosecond isolated soft X-ray pulse generation is possible using CEP stable, two-color laser fields.

4. Conclusion

In summary, we have investigated and optimized HHG in a 790 nm+1300 nm two-color field. At the overlap of the two pulses, a broad continuum is generated up to photon energies exceeding 160 eV, representing a clear extension compared to HHG with a single NIR pulse. By combining a long cell and a high gas pressure, we demonstrate a high flux across a wide spectral region. Due to the large interaction volume with favorable PM conditions, it is possible to partially compensate for the reduced single-atom response at the longer-wavelength driving fields. Numerical simulations suggest that hybrid optical and PM gating selects attosecond emission bursts that are formed after a few mm propagation in the gas cell. With two-color pulses, PM for a coherent build-up along the cell enables control of the temporal profile of the soft X-ray bursts, and ultimately should allow to generate isolated attosecond pulses with high flux and high photon energies. The approach presented in this paper can be generalized to the use of longer MIR wavelengths, permitting increase of the HHG cut-off to the water window and allowing core-shell photoelectron and transient absorption techniques to access the K-edge of carbon, nitrogen and oxygen atoms.

Acknowledgments

The project was partially supported by the Hungarian Scientific Research Fund (OTKA project NN107235). KV acknowledges support from the Bolyai Grant of the Hungarian Academy of Sciences. AR and MV acknowledge support from the Deutsche Forschungsgemeinschaft (DFG-ERA Grant VR 76/1-1 and DFG Grant RO 4577/1-1). KK and TV acknowledge support from the projects PN-II-RU-PD-2011-3-0236 and PN-II-ID-PCE-2012-4-0342.

#248407 Received 24 Aug 2015; revised 16 Nov 2015; accepted 16 Nov 2015; published 23 Dec 2015